Comparative Study of Burr-XII Nested Hazard Models: Simulation under Mixed Directional Effects and AML Data Analysis

Sahar Dalvand[1], Amir Kasaeian[2,3,4], Mohammad Vaezi[5,6], Shahrbano Rostami[6], Hojjat Zeraati[1,*,#] and Mehdi Yaseri[1,*,#]

[1]*Department of Epidemiology and Biostatistics, School of Public Health, Tehran University of Medical Sciences, Tehran, Iran*

[2]*Liver and Pancreatobiliary Diseases Research Center, Digestive Diseases Research Institute, Tehran University of Medical Sciences, Tehran, Iran*

[3]*Digestive Oncology Research Center, Digestive Diseases Research Institute, Tehran University of Medical Sciences, Tehran, Iran*

[4]*Research Center for Chronic Inflammatory Diseases, Tehran University of Medical Sciences, Tehran, Iran*

[5]*Hematology, Oncology, and Stem Cell Transplantation Research Center, Research Institute for Oncology, Hematology, and Cell Therapy, Tehran University of Medical Sciences, Tehran, Iran*

[6]*Cell Therapy and Hematopoietic Stem Cell Transplantation Research Center, Research Institute for Oncology, Hematology and Cell Therapy, Tehran University of Medical Sciences, Tehran, Iran*

Abstract: Choosing an appropriate hazard-based regression model is critical in survival analysis. The proportional hazards (PH), accelerated failure time (AFT), and accelerated hazard (AH) models make distinct assumptions about covariate effects, yet real data often violate these assumptions. The general hazard (GH) model nests all three frameworks, allowing both time-scale and hazard-scale effects within a single structure. This paper presents a comparative study of the four nested models (PH, AFT, AH, GH) using the three-parameter Burr XII baseline hazard. Extensive simulations under ten scenarios, including both positive and negative covariate effects, evaluate maximum likelihood estimators via bias, standard errors, mean squared error, coverage probability, and information criteria. Sample sizes of 1000 and 5000 with 20% and 40% censoring are considered. A dedicated simulation examines the recovery of increasing, decreasing, and unimodal hazard shapes. Results show that the GH model consistently recovers the true data-generating structure and all three hazard patterns. The GH model yields the lowest information criterion values among its submodels, supporting its utility as a data-driven model selection tool. Practical relevance is illustrated using real survival data from 801 acute myeloid leukemia (AML) patients who received allogeneic stem cell transplantation. This comparative framework offers applied researchers a systematic, evidence-based approach to select the most appropriate hazard structure for right-skewed, heavily censored survival data.

Keywords: General hazard, Burr XII, Hazard function, Parametric model, AML, Maximum likelihood.

1. INTRODUCTION

Survival data analysis is often complicated by censoring and time-varying hazard rates. Managing diverse hazard patterns is a challenge, as conventional models may fail to capture complex characteristics, particularly when covariate effects change over time or show non-proportional influences. Hazard-based regression models are essential for quantifying the relationship between covariates and the baseline hazard function (BHF). Three main frameworks are the Cox proportional hazards (PH) model, the accelerated failure time (AFT) model, and the accelerated hazard (AH) model. Each has its assumptions, strengths, and limitations. The semiparametric Cox PH model is widely used due to its simplicity, assuming covariates have a multiplicative, time-constant effect on the hazard. However, violations of the PH assumption can lead to misleading results. The AFT model directly models survival time and accommodates non-proportional effects, while the AH model allows non-proportional covariate effects and identical hazards at t=0, making it suitable for crossing survival curves. Nevertheless, none of these three models can simultaneously handle covariates with proportional and time-independent effects alongside those with non-proportional and time-dependent effects in a single analysis [1].

The general hazard (GH) regression model, originally formulated by Chen and Jewell [2] and further developed in parametric settings by Rubio *et al*. [1], provides a unified framework that nests the PH, AFT, and AH models. This model allows some covariates to have proportional (time-independent) effects while others have non-proportional (time-dependent) effects within the same model a feature not available in the three classic submodels.

The primary objectives of this paper are twofold. First, we conduct a comprehensive comparative study of the four nested hazard models (PH, AFT, AH, and GH) under the Burr XII baseline using maximum

*Address correspondence to this author at the Department of Epidemiology and Biostatistics, School of Public Health, Tehran University of Medical Sciences, Tehran, Iran; E-mail: zeraatih@tums.ac.ir, m.yaseri@gmail.com

#These authors contributed equally.

likelihood estimation. Unlike previous simulation studies [1, 3] that focused mainly on positive covariate effects and larger sample sizes, our simulation design explicitly includes both positive and negative regression coefficients (mixed effects) and considers smaller sample sizes (n=1000 and 5000) with censoring rates of 20% and 40%. Additionally, we examine the model's ability to recover increasing, decreasing, and unimodal hazard patterns under light to heavy censoring. We evaluate estimator performance across ten distinct simulation scenarios, covering a wide range of data generating structures. Performance metrics include bias, empirical and model-based standard errors, mean squared error, root mean squared error, coverage probability of 95% confidence intervals, and information criteria (AIC, AICc, BIC, HQIC).

Second, we apply the proposed comparative framework to a real-world acute myeloid leukemia (AML) dataset of 801 patients who underwent allogeneic stem cell transplantation. This allows us to illustrate how the nested structure of the GH model can serve as a practical, data-driven tool for selecting the most appropriate hazard structure (PH, AFT, AH, or GH) for a given dataset. The AML context is clinically relevant, as post-transplant survival is influenced by time-dependent factors such as disease status and graft-versus-host disease.

Several parametric extensions of the GH model have been proposed in the literature [1, 3]. Rubio *et al*. [1] introduced a general hazard structure for excess mortality modeling, and subsequent work has explored various baseline distributions. Although the Burr XII distribution is a special case of the generalized log-logistic distribution, the present study focuses specifically on the practical comparative behavior of the nested hazard models under a Burr XII baseline including hazard shape recovery, robustness under misspecification, and finite‐sample performance. In this context, the present study distinguishes itself by offering a dedicated, in-depth comparison of the four nested hazard models under the Burr XII distribution, with particular attention to four aspects that have received limited attention in previous comparative studies: (i) the inclusion of both positive and negative covariate effects in simulation scenarios; (ii) the use of a wide range of evaluation metrics across ten distinct scenarios including smaller sample sizes (n=1000); (iii) validation on a clinically relevant AML dataset that differs from previously analyzed cancer data; and (iv) a dedicated simulation study based on different hazard shapes increasing, decreasing, and unimodal which has not been performed in previous GH-based research. By focusing on the comparative evaluation rather than introducing a new model, this paper aims to provide applied researchers with a clear, evidence-based guide for choosing among PH, AFT, AH, and GH structures when the baseline hazard is assumed to follow a Burr XII distribution.

The remainder of this paper is organized as follows. Section 2 reviews the GH model formulation and the Burr XII distribution. Section 3 presents the maximum likelihood inference procedures, including asymptotic properties and identifiability considerations. Section 4 describes the data generation and evaluation metri. Section 5 reports the simulation design. Section 6 reports the simulation results assessing the MLE estimators' performance. Section 7 applies the models to AML data. Sections 8 and 9 contain discussion and conclusions. Sections 10 and 11 cover data availability and declarations.

2. METHOD

2.1. General Hazard Model Formulation

Assuming that x is a vector of the covariates, T is the positive time to event random variable, and $\exp\{\boldsymbol{X}'\beta\}$ is the covariate link function, the hazard function (h_{GH}), cumulative hazard function (H_{GH}), survival function (S_{GH}), probability density function f_{GH} (PDF), and the cumulative distribution function F_{GH} (CDF) of the GH model is written as follows:

$$h_{GH}(t;\beta_1,\beta_2,x) = h_0(t\exp\{x'\beta_1\})\exp\{x'\beta_2\} \quad (1)$$

$$H_{GH}(t;\beta_1,\beta_2,x) = H_0(t\exp\{x'\beta_1\})\exp\{x'(\beta_2-\beta_1)\} \quad (2)$$

$$S_{GH}(t;\beta_1,\beta_2,x) = S_0(t\exp\{x'\beta_1\})\exp\{x'(\beta_2-\beta_1)\} \quad (3)$$

$$f_{GH}(t;\beta_1,\beta_2,x) = h_0(t\exp\{x'\beta_1\})\exp\{x'\beta_2\}S_0(t\exp\{x'\beta_1\})\exp\{x'(\beta_2-\beta_1)\} \quad (4)$$

$$F_{GH}(t;\beta_1,\beta_2,x) = 1 - S_{GH}(t;\beta_1,\beta_2,x) = 1 - S_0(t\exp\{x'\beta_1\})\exp\{x'(\beta_2-\beta_1)\} \quad (5)$$

where β_1 and β_2 are the unknown regression parameters of the model; h_0, H_0 , and S_0 are the baseline hazard, cumulative hazard, and survival function, respectively; independent covariate $x=(x_1,x_2,\dots,x_p)^T$; the $h_0(t)$ is BHF for a case in which all independent covariates are equal to zero; $\beta=(\beta_1,\beta_2,\dots,\beta_p)^T$ is the vector of regression coefficients; $\exp\{x'_j\beta\}$ represents the hazard ratio due to a one-unit increase in the jth covariate.

2.2. Burr XII Distribution

In 1942, twelve different forms of distribution functions for modeling lifetime data were introduced by

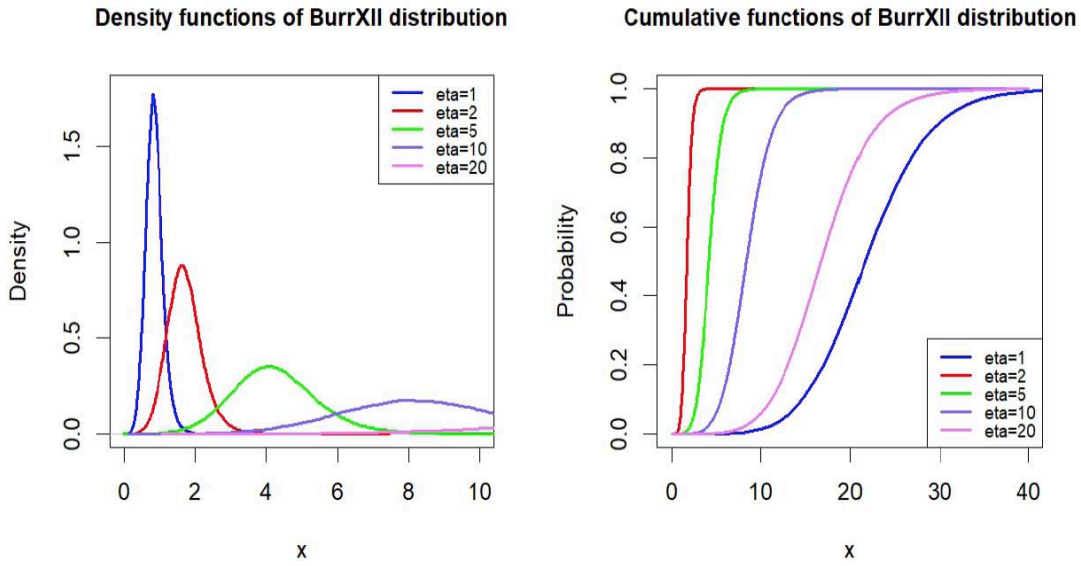

Figure 1: Different densities and cumulative functions of Burr XII ($\eta,\ \nu,\ \delta$) distribution with different values of η and fixed values of ν=5 and δ=2.

Burr, of which the type XII distribution has been the most popular. The three-parameter BXII distribution models a wide range of data, particularly in survival analysis and reliability modeling. Based on the values of its shape and scale parameters, it includes several well-known distributions as special cases, such as gamma, log-normal, and logistic distributions, and two asymptotic cases, Weibull and Pareto Type I [4]. Due to its three-parameter nature, with two shape parameters, it can capture various risk functions and cover a wide range of skewness and kurtosis values [4]. Figure **1** shows different PDFs and CDFs of the BXII distribution for different values of η , ν, and δ, respectively. According to Figure **1**, as the scale parameter η increases, the shape of the BXII PDF with constant values of ν and δ becomes flatter.

The CDF of the BXII distribution is expressed as:

$$F_{BXII}\left(t;\ \nu,\delta,\eta\right)=1-\left(1+\left(\frac{t}{\eta}\right)^{\nu}\right)^{-\delta}\quad(6)$$

The PDF of the BXII distribution is expressed as follows:

$$f_{BXII}\left(t;\ \nu,\delta,\eta\right)=\frac{\nu\delta}{\eta}\left(\frac{t}{\eta}\right)^{\nu-1}\left(1+\left(\frac{t}{\eta}\right)^{\nu}\right)^{-(\delta+1)}\quad(7)$$

The SF of the BXII distribution is computed as follows:

$$S_{BXII}\left(t;\ \nu,\delta,\eta\right)=\left(1+\ (\frac{t}{\eta})^{\nu}\right)^{-\delta}\quad(8)$$

The HF of the BXII distribution is expressed as follows:

$$h(t)=\frac{\nu\delta}{\eta}\left(\frac{t}{\eta}\right)^{\nu-1}\left(1+\left(\frac{t}{\eta}\right)^{\nu}\right)^{-1}\quad(9)$$

The CHF of the BXII distribution is:

$$H_0(t)=\delta\ log\left(1+\ (\frac{t}{\eta})^{\nu}\right)\ (10)$$

Where t>0 is the support of the distribution.

2.3. BXII GH Model

For the GH model, based on equation (12), the hazard function for a person with the covariate x is computed as follows:

$$h_{GH-BXII}\left(t;\boldsymbol{\psi},\boldsymbol{\beta}_1,\boldsymbol{\beta}_2\right)=\frac{\nu\delta}{\eta}\left(\frac{t\exp\{x'\beta_1\}}{\eta}\right)^{\nu-1}\left(1+\left(\frac{t\exp\{x'\beta_1\}}{\eta}\right)^{\nu}\right)^{-1}\exp\{x'\beta_2\}\ (11)$$

where $\boldsymbol{\psi}$ is the vector of the distribution parameters. The CHF of the BXII distribution of the GH model is as follows:

$$H_{GH-BXII}\left(t;\boldsymbol{\psi},\boldsymbol{\beta}_1,\boldsymbol{\beta}_2\right)=\delta\ log\left(1+\ (\frac{t\exp\{x'\beta_1\}}{\eta})^{\nu}\right)\exp\{x'(\beta_2-\beta_1)\}\ (12)$$

The SF of the BXII distribution of the GH model is as follows:

$$S_{GH-BXII}\left(t;\boldsymbol{\psi},\boldsymbol{\beta}_1,\boldsymbol{\beta}_2\right)=\left(1+\ (\frac{t\exp\{x'\beta_1\}}{\eta})^{\nu}\right)^{-\delta}\exp\{x'(\beta_2-\beta_1)\}\ (13)$$

3. MODEL INFERENCE

Two methods are commonly used to estimate the distribution parameters of the BXII, which are:

1. Standard BXII distribution tables;
2. Maximum likelihood estimation (MLE) approach.

This section discusses the classical approach by estimating the maximum likelihood (ML) for hazard-based regression models with the BXII BHF. To estimate the model's parameters using the frequentist method, we assume that the time to event data are skewed to the right and have non-informative censorship. In this regard, the censored likelihood function can be defined as follows:

$$L(\boldsymbol{\psi}, \beta_1, \beta_2; D) = \prod_{i=1}^{n} \left[h_0(t_i, \eta, \nu, \delta) e^{x_i' \beta 2}\right]^{\sigma_i} \exp\left[-H_0(t_i, \eta, \nu, \delta) e^{x_i' \beta_2 - x_i' \beta_1}\right]$$

$$= \prod_{i=1}^{n} \left[h_0\left(t_i \exp\left\{x'_i \beta_1, \boldsymbol{\psi}\right\}\right) \exp\{x'_i \beta_2\}\right]^{\sigma_i} \times \quad (14)$$

$$exp\left[-H_0\left(t_i \exp\left\{x'_i \beta_1, \boldsymbol{\psi}\right\}\right) \exp\{x'_i \beta_2 - x'_i \beta_1\}\right]$$

Where D represents the observed data (t_i=survival time and x_i=covariates) and σ_i , represents the censoring rate, which includes 0 and 1, where 0 is equivalent to censorship, and 1 is equivalent to the event's occurrence. Now, according to the HF and CHF presented in equations 12 and 13, the logarithm of the likelihood function of the GH-BXII model is expressed as follows:

$$\ell\left(\boldsymbol{\psi}, \beta_1, \beta_2; D\right) = \sum_{i=1}^{n} \sigma_i \log h_0(t) + \sum_{i=1}^{n} \sigma_i x'_i \beta_2 - \sum_{i=1}^{n} H_0(t_i) e^{x'_i \beta_2} - \sum_{i=1}^{n} x'_i \beta_1 =$$

$$\sum_{i=1}^{n} \sigma_i \log(\nu) + \sum_{i=1}^{n} \sigma_i \log(\delta) - \sum_{i=1}^{n} \sigma_i \log(\eta) + \sum_{i=1}^{n} \sigma_i (\nu - 1) \log\left(\frac{t_i e^{x'_i \beta_1}}{\eta}\right) - \sum_{i=1}^{n} \sigma_i \log\left(1 + \left(\frac{t_i e^{x'_i \beta_1}}{\eta}\right)^{\nu}\right) + \sum_{i=1}^{n} \sigma_i \, x'_i \beta_2 - \quad (15)$$

$$\sum_{i=1}^{n} \delta \; log\left(1 + \left(\frac{t_i e^{x'_i \beta_1}}{\eta}\right)^{\nu}\right) e^{x'_i \beta_2 - x'_i \beta_1}$$

$$\frac{\partial \ell}{\partial \eta} = \sum_{i=1}^{n} \sigma_i \left(-\frac{1}{\eta} + \frac{\nu \left(\frac{t_i e^{x'_i \beta_1}}{\eta}\right)^{\nu}}{\eta\left(1 + \left(\frac{t_i e^{x'_i \beta_1}}{\eta}\right)^{\nu}\right)}\right) - \sum_{i=1}^{n} \frac{\delta \nu \left(\frac{t_i e^{x'_i \beta_1}}{\eta}\right)^{\nu}}{\eta\left(1 + \left(\frac{t_i e^{x'_i \beta_1}}{\eta}\right)^{\nu}\right)} \; e^{x'_{i(\beta_2 - \beta_1)}}$$

$$= -\frac{\nu}{\eta} \sum_{i=1}^{n} \left(\frac{\sigma_i}{1 + \left(\frac{t_i e^{x'_i \beta_1}}{\eta}\right)^{\nu}}\right) + \frac{\delta \nu}{\eta} \sum_{i=1}^{n} \frac{\left(\frac{t_i e^{x'_i \beta_1}}{\eta}\right)^{\nu}}{1 + \left(\frac{t_i e^{x'_i \beta_1}}{\eta}\right)^{\nu}} e^{x'_{i(\beta_2 - \beta_1)}} \quad (16)$$

$$\frac{\partial \ell}{\partial \nu} = \sum_{i=1}^{n} \sigma_i \left(\frac{1}{\nu} + log\,(t_i) - \log(\eta) + x'_i \beta_1 - \frac{\left(\frac{t_i e^{x'_i \beta_1}}{\eta}\right)^{\nu} \log\left(\frac{t_i e^{x'_i \beta_1}}{\eta}\right)}{1 + \left(\frac{t_i e^{x'_i \beta_1}}{\eta}\right)^{\nu}}\right) -$$

$$\sum_{i=1}^{n} \delta \frac{\left(\frac{t_i e^{x'_i \beta_1}}{\eta}\right)^{\nu} \log\left(\frac{t_i e^{x'_i \beta_1}}{\eta}\right)}{1 + \left(\frac{t_i e^{x'_i \beta_1}}{\eta}\right)^{\nu}} \; e^{x'_{i(\beta_2 - \beta_1)}} \quad (17)$$

$$\frac{\partial \ell}{\partial \delta} = \sum_{i=1}^{n} \sigma_i \left(\frac{1}{\delta} - \log\left(1 + \left(\frac{t_i e^{x'_i \beta_1}}{\eta}\right)^{\nu}\right)\right) - \sum_{i=1}^{n} log\left(1 + \left(\frac{t_i e^{x'_i \beta_1}}{\eta}\right)^{\nu}\right) e^{x'_{i(\beta_2 - \beta_1)}} \quad (18)$$

$$\frac{\partial \ell}{\partial \beta_{1,j}} = \sum_{i=1}^{n} \sigma_i \left((\nu - 1) x_{ij} - \frac{\nu \left(\frac{t_i e^{x'_i \beta_1}}{\eta}\right)^{\nu} x_{ij}}{1 + \left(\frac{t_i e^{x'_i \beta_1}}{\eta}\right)^{\nu}}\right) - \sum_{i=1}^{n} \delta \frac{\nu \left(\frac{t_i e^{x'_i \beta_1}}{\eta}\right)^{\nu} x_{ij}}{1 + \left(\frac{t_i e^{x'_i \beta_1}}{\eta}\right)^{\nu}} e^{x'_{i(\beta_2 - \beta_1)}} \quad (19)$$

$$\frac{\partial \ell}{\partial \beta_{2,j}} = \sum_{i=1}^{n} \delta_i \, x_{ij} - \sum_{i=1}^{n} \delta \, x_{ij} e^{x'_{i(\beta_2 - \beta_1)}} \quad j=1,2,\ldots,p. \quad (20)$$

By refining the initial partial derivatives, the maximum likelihood estimates (MLE) for the unknown distribution parameters ψ'^*=(η, ν, δ) and the model's regression coefficients (β_1, β_2) are obtained by solving a system of nonlinear equations of $\frac{\partial \ell}{\partial \eta} = 0$, $\frac{\partial \ell}{\partial \nu} = 0$, $\frac{\partial \ell}{\partial \delta} = 0$, $\frac{\partial \ell}{\partial \beta_{1,j}} = 0$, and $\frac{\partial \ell}{\partial \beta_{1,j}} = 0$, iteratively. To achieve accurate parameter estimates, we employed robust optimization methods. In particular, we used R's nlminb function, which is well-suited for handling intricate optimization problems efficiently. With increasing sample sizes, MLE approximate a normal distribution. This enables us to perform hypothesis tests and construct confidence intervals for the model's distributional parameters, like shape and scale, as well as its regression coefficients.

3.1. Asymptotic Properties of the Maximum Likelihood Estimators

Under the standard regularity conditions for parametric survival models with right-censored data (i.i.d. observations, true parameter in the interior of the parameter space, twice-differentiable log-likelihood, and a non-singular Fisher information matrix), the MLEs of the GH-BXII model satisfy the following large-sample properties.

Consistency: As the sample size *n* increases, the MLE $\hat{\psi}$=($\hat{\eta}$, $\hat{v}$, $\hat{\delta}$, $\hat{\beta_1}$, $\hat{\beta_2}$) converges in probability to the true parameter vector $\hat{\psi} \xrightarrow{p} \psi_0$. This is empirically supported by our simulations (Tables **1-4**), where bias decreases and RMSE improves when n increases from 1000 to 5000.

Asymptotic normality: The MLE is asymptotically normally distributed:

$$\sqrt{n}(\hat{\psi} - \psi_0) \xrightarrow{d} N_{P+3}(0, I(\psi_0)^{-1})$$

where $I(\psi_0)$ is the expected Fisher information matrix. Because the expected information matrix has no closed form due to the complexity of the GH-BXII log-likelihood, we use the observed Fisher information matrix for inference:

$$I_{obs}(\hat{\psi}) = -\frac{\partial^2 \ell(\psi, D)}{\partial\psi\partial\psi^T} |\psi = \hat{\psi}.$$

The inverse of $I_{obs}(\hat{\psi})$ provides a consistent estimator of the asymptotic covariance matrix. The model-based standard errors (M.SE) reported in Tables **1-4** are obtained from this matrix. Coverage probabilities close to the nominal 95% level (especially for *n*=5000) empirically validate the normal approximation.

Asymptotic efficiency: Among all regular and consistent estimators, the MLE achieves the smallest asymptotic variance (Cramér-Rao lower bound). The reduction in empirical standard deviation (E.SD) with increasing sample size (e.g., for *η* from 0.105 *n*=1000 to 0.047 at *n*=5000 in Table **1**) demonstrates this efficiency.

To empirically assess numerical stability, we examined the observed Hessian matrix (the negative of the second derivatives of the log-likelihood) evaluated at the MLE for all simulation replicates. As reported in Supplementary Table **S21**, the proportion of replicates with a positive definite Hessian (and hence an operationally invertible observed Fisher information matrix) is provided for each scenario, sample size, and censoring level. Under 40% censoring, this proportion ranged from 95.41% to 99.23%, with the highest values observed under correct model specification (GH1-GH). For correctly specified models, the Hessian was positive definite in at least 98% of replicates across all censoring levels. Overall, these results indicate a high degree of numerical stability and suggest that asymptotic standard errors and Wald-type confidence intervals are well-defined for the vast majority of simulation replicates.

3.2. Parameter Identifiability

A concern with flexible general hazard models is whether all parameters can be uniquely determined from the observed data, especially when both time-scale (β_1) and hazard-scale (β_2) regression coefficients are estimated together with three baseline Burr XII parameters (η, v, *δ*). The proposed GH-BXII model is practically identifiable for the following reasons.

Structural Separation: The hazard function (14) shows that β_1 operates inside the argument t exp{x′ β_1} (affecting the time scale), while β_2 appears as a multiplicative factor exp{x′ β_2}. This structural distinction prevents exact confounding between the two regression vectors. The three nested submodels (PH, AFT, AH) are obtained by setting specific constraints ($\beta_1 = 0$, $\beta_2 = 0$, or $\beta_1 = \beta_2$), which further anchors the parameter space.

Empirical Evidence: Convergence rates were generally high across all simulation scenarios. As detailed in Supplementary Table **S21**, for correctly specified models (GH1-GH), convergence exceeded 98.9% in all scenarios and reached 99.7% for n=5000 with 20% censoring. Under misspecification (data generated from PH, AFT, or AH structures and fitted with the GH model), convergence rates ranged from 95.83% to 99.43%. Non-convergent replicates were excluded from subsequent performance evaluations.

Furthermore, the information criterion comparisons (Tables **S2-S5** in the supplementary material) show that when data were generated from a specific submodel (PH, AFT, or AH), that same submodel (or the full GH model) was consistently identified as the best-fitting. This ability to recover the true data generating structure confirms structural identifiability.

Practical Caution: While identifiability holds for moderate to large samples (*n*≥1000) and censoring rates up to 40%, small samples (*n*<500) or very heavy censoring (>60%) may lead to unstable estimates, particularly for the shape parameter *v* (see Table **1**, coverage 91% at *n*=1000, 40% censoring). In such settings, we recommend first fitting the simpler nested models (PH, AFT, AH) and using likelihood ratio tests or information criteria to decide whether the full GH model is necessary. This pragmatic approach mitigates any weak identifiability issues.

4. DATA GENERATION

Survival data for GH, PH, AFT, and AH models were generated using the inverse transformation method, which utilizes R software based on the relationship between the cumulative hazard function and a uniform random variable. In this regard, the method of Bender *et al.* [5] was used to simulate the survival data for the Cox PH model, while the method

of Leemis *et al.* was employed for the AFT model, and the same method as AFT was applied to the AH and GH models [6].

For the GH model, survival data are generated using the following formula:

$$\mathrm{T} = \frac{1}{\exp(x'\beta_1)} \mathrm{H}_0^{-1}\left(\frac{-\log(1-U)}{\exp(x'\beta_2 - x'\beta_1)}\right)$$

For the PH structure of the formula: $T = H_0^{-1}\left(\frac{-log\,(1-U)}{exp(x'\beta)}\right)$; for the AFT model of the formula: $T = \frac{H_0^{-1}\{-log\,(1-U)\}}{exp(x'\beta)}$; And for the AH model, the following formula is used:

$$\mathrm{T} = \frac{1}{\exp(x'\beta)} \mathrm{H}_0^{-1}\left(-\frac{\log(1-U)}{\exp(x'\beta)}\right)$$

Where H_0^{-1} is equivalent to the inverse of the CHF, the inverse of the desired BXII distribution. This study conducted a series of simulations to evaluate the effect of sample size and censoring rate from light to heavy censoring cases. Continuous covariate age was generated using a normal distribution with a mean of 50 and a standard deviation of 9 years; gender and treatment were also generated using a binomial distribution with a probability of 0.5 as binary covariates, referring to the scenario of the cancer dataset from studies [1, 3, 7, 8].

4.1. Evaluation Metrics

This study aims to demonstrate how the proposed model's nested structure compares with the most commonly used parametric approaches for survival data analysis. The Akaike information criterion

(AIC), corrected Akaike information criterion (AICc), Bayesian information criterion (BIC), and the Hannan–Quinn information criterion (HQIC) have also been utilized to select the model that best fits the data based on the desired structure and effectively illustrate the effects of sample size and censoring rate.

5. SIMULATION SCENARIOS

This section uses various simulation scenarios to demonstrate the proposed model's inferential characteristics, model estimator performance, nesting structure, and suitability. Based on this, the following section examines the classical approach of the GH model and its sub-models. In all scenarios, the survival time data were analyzed using the GH structure with the BXII distribution of BHF, under data generated by the GH, PH, AFT, and AH structures, respectively.

5.1. Scenario 1

This simulation study was designed to comprehensively compare four widely used survival modeling frameworks under various hazard structures, including the GH, PH, AFT, and AH structure models. The baseline hazard in all data generating processes was specified using the BXII distribution, parameterized by shape parameters (η and ν) and scale parameter (δ). Survival times were simulated under ten distinct scenarios (GH-1 to GH-4, PH-1 to PH-2, AFT-1 to AFT-2, AH-1 to AH-2), each reflecting the structural assumptions of the corresponding model class. Three covariates were included: age (X_1), sex (X_2), and treatment (X_3), with true regression parameters specified separately for hazard and time components, as summarized in supplementary Table **S1**. The design incorporated positive, negative, and mixed covariate effects to ensure a broad spectrum of evaluation conditions. Both administrative and random censoring mechanisms were applied to approximate realistic clinical settings. Administrative censoring was fixed at T_c=5, while additional censoring times were generated from an exponential distribution with rate parameters (r) calibrated to yield approximately 20% and 40% censoring, with the corresponding values provided in Table **S1**. To balance precision with computational feasibility, the primary scenarios (GH-1, PH-1, AFT-1, AH-1) were replicated N=10000 times at sample sizes n=1000 and n=5000. In contrast, the complementary scenarios (GH-2, GH-3 and GH-4, PH-2, AFT-2, AH-2) were run with N=1000 replications to explore alternative effect patterns while maintaining efficiency. The primary objective was to assess model performance when the fitted model corresponded to the data-generating mechanism and to evaluate the consequences of model misspecification, with performance judged based on bias, empirical standard deviation, mean squared error, root mean squared error, and the coverage probability of 95% confidence intervals.

5.2. Scenario 2

To further illustrate the flexibility of the GH-BXII model, we conducted an additional simulation study focusing on the shape of the hazard function. Specifically, we generated data under three distinct hazard patterns: increasing, decreasing, and unimodal hazards. For each scenario, survival times were simulated from the GH-BXII distribution, and the corresponding MLEs were obtained. For each case, data were generated with sample sizes of 1000 and 5000 with N=1000 replications, T_c=10 and r=0.5 which induced approximaley 20% censoring, T_c=10 and r=1.3 which induced approximaley 40% censoring for unimodal hazard; T_c=10 and r=0.1 which induced

approximaley 20% censoring, T_c=10 and r=0.5 which induced approximaley 40% censoring for decreasing hazard; T_c=10 and r=0.1 which induced approximaley 20% censoring, T_c=5 and r=0.40 which induced approximaley 40% censoring for increasing hazard. This additional simulation aims not to reassess estimator properties such as coverage but to demonstrate the model's ability to accommodate different hazard shapes.

6. RESULT

6.1. Scenario 1 Results

The GH–BXII model consistently provided the best fit to the simulated data in the GH structure, yielding the lowest AIC, BIC, AICc, and HQIC values across both sample sizes and censoring rates (Table **S2**). At lower censoring (20%), the AFT–BXII model outperformed the PH–BXII and AH–BXII models based on information criteria; however, at higher censoring (40%), the PH–BXII model surpassed the AFT–BXII, while the AH–BXII model consistently showed the weakest fit with the highest information criteria values. Parameter recovery further confirmed the superiority of the GH–BXII model. With n=1000 and 20% censoring, bias for η was –0.043 and for ν nearly zero (0.004), with coverage close to 95%. The scale parameter δ, however, was slightly underestimated (bias –0.091, RMSE 0.174). Increasing the sample size from 1000 to 5000 reduced variability substantially: the RMSE for η declined from 0.114 to 0.051, and for δ from 0.174 to 0.077.

Furthermore, we also evaluated the performance of MLEs under three other generalized hazard structures (GH-2, GH-3, and GH-4) using the BXII baseline hazard with sample sizes of 1,000 and 5,000 and censoring rates of 20% and 40%. Across all structures, the MLEs of the baseline parameters (η, ν, δ) and regression coefficients (β) showed low bias, adequate coverage, and satisfactory RMSE, indicating that the estimators were generally accurate and consistent. Increasing the sample size improved precision and reduced variability, while higher censoring slightly increased the bias and RMSE, particularly for the shape parameter (supplementary Tables **S6-S11**). These results highlight the robustness of the GH–BXII model in terms of both model selection criteria and parameter estimation, while also showing that the AFT and PH models can provide reasonable approximations depending on censoring, and the AH model fits the data poorly under this scenario.

For the PH-1 structure (PH-generated data), the PH-BXII model showed the strongest performance, demonstrating the lowest values in all information measures (Table **S3**). According to model selection criteria, the GH model emerged as the optimal choice for PH-1 and PH-2 structural frameworks in larger sample sizes, with the PH model ranking second. The PH–BXII model consistently provided more efficient covariate effect estimation than GH–BXII (Table **2**). For example, at n=1000 with 20% censoring, the RMSE for the treatment effect (β_3) was 0.072 under PH–BXII compared with 0.084 under GH–BXII. Coverage probabilities were generally close to the nominal 95%, though the shape parameter ν showed some under-coverage (as low as 92% at n=5000 and 40% censoring). Furthermore, comprehensive details of the PH-2 structure model fit for the PH and GH models are provided (supplementary Tables **S12-S14**).

A notable finding from the simulation study is that when data were generated under the PH-1 structure, the GH-BXII model correctly recovered the null time-scale component. Specifically, the coefficients β_{11}, β_{12}, and β_{13} which are zero in the true model were estimated with means essentially equal to zero. This demonstrates that the flexible GH framework does not spuriously introduce time-scale effects when the true underlying structure is purely proportional hazards, confirming the model's ability to collapse to its nested sub-models when appropriate.

In the AFT-1 structure of the AFT-BXII scenario, model comparison based on information criteria showed that the AFT–BXII model provided the best overall fit to the simulated data, with the GH–BXII model consistently ranking second (supplementary Table **S4**). This finding is consistent with the theoretical relationship between the two frameworks, where the AFT model is a special case of the GH model. Quantitatively, the AFT–BXII model demonstrated minimal bias and the lowest RMSE in recovering time-scale parameters; for example, at n=1000 with 20% censoring, bias in β_1 was virtually zero with an RMSE of 0.027, compared with 0.064 under GH–BXII. The GH–BXII model also performed reasonably well but showed a larger bias in the scale parameter (δ=−0.081). As expected, increasing the sample size improved precision considerably, with RMSEs for regression coefficients dropping below 0.03 at n=5000. Under the AFT-1 scenario, the GH-BXII model correctly recovered the expected equivalence between the time-scale and hazard-scale effects. In particular, the estimated coefficients on the two scales were nearly identical across covariates, so that $\widehat{\beta_2} - \widehat{\beta_1}$ was close to zero. For example, for age, $\widehat{\beta_{11}}$=0.10 and $\widehat{\beta_{21}}$=0.10. This agrees with the structural constraint of the AFT model nested within the GH framework and confirms that the proposed model does not induce spurious departures from the true AFT structure.

Table 1: Simulation from the GH-1 Structure with (η, ν, δ) = (1.25, 2.45, 1.15), β_t = (0.25, 0.35, 0.15), β_h = (0.15, 0.10, 0.25)

$h_{BXII}^{GH}(t; x_j) = h_{BXII}(t \times \exp(0.10 \times age + 0.15 \times sex + 0.20 \times TRT)\,; 1.45, 2.10, 1.15) \times \exp(\,0.10 \times age + 0.15 \times sex + 0.20 \times TRT).$

Model	Parameters	TRUE	M.MLE	m.MLE	E.SD	M.SE	Coverage	Bias	MSE	RMSE
n=1000, 20% Censoring										
GH-BXII	η	1.250	1.207	1.201	0.105	0.118	0.957	-0.043	0.013	0.114
	ν	2.450	2.454	2.453	0.042	0.052	0.983	0.004	0.002	0.043
	δ	1.150	1.059	1.042	0.148	0.185	0.970	-0.091	0.030	0.174
	β_{11}	0.250	0.246	0.246	0.051	0.052	0.953	-0.004	0.003	0.051
	β_{12}	0.350	0.349	0.348	0.103	0.104	0.952	-0.001	0.011	0.103
	β_{13}	0.150	0.143	0.144	0.101	0.102	0.953	-0.007	0.010	0.101
	β_{21}	0.150	0.154	0.154	0.040	0.040	0.947	0.004	0.002	0.040
	β_{22}	0.100	0.105	0.105	0.081	0.079	0.944	0.005	0.007	0.081
	β_{23}	0.250	0.252	0.252	0.080	0.078	0.950	0.002	0.006	0.080
n=1000, 40% Censoring										
GH-BXII	η	1.250	1.252	1.234	0.157	0.151	0.948	0.002	0.025	0.157
	ν	2.450	2.431	2.430	0.063	0.057	0.911	-0.019	0.004	0.066
	δ	1.150	1.134	1.095	0.245	0.246	0.963	-0.016	0.060	0.245
	β_{11}	0.250	0.249	0.249	0.064	0.064	0.953	-0.001	0.004	0.064
	β_{12}	0.350	0.352	0.351	0.128	0.129	0.955	0.002	0.016	0.128
	β_{13}	0.150	0.150	0.150	0.127	0.126	0.951	0.000	0.016	0.127
	β_{21}	0.150	0.151	0.151	0.052	0.052	0.950	0.001	0.003	0.052
	β_{22}	0.100	0.101	0.101	0.106	0.103	0.943	0.001	0.011	0.106
	β_{23}	0.250	0.247	0.247	0.103	0.100	0.948	-0.003	0.011	0.103
n=5000, 20% Censoring										
GH-BXII	η	1.250	1.228	1.227	0.047	0.053	0.961	-0.022	0.003	0.051
	ν	2.450	2.471	2.470	0.019	0.023	0.908	0.021	0.001	0.028
	δ	1.150	1.112	1.110	0.068	0.085	0.970	-0.038	0.006	0.077
	β_{11}	0.250	0.248	0.248	0.022	0.023	0.953	-0.002	0.001	0.023
	β_{12}	0.350	0.347	0.347	0.045	0.046	0.956	-0.003	0.002	0.045
	β_{13}	0.150	0.149	0.150	0.044	0.046	0.959	-0.001	0.002	0.044
	β_{21}	0.150	0.151	0.151	0.018	0.018	0.952	0.001	0.000	0.018
	β_{22}	0.100	0.101	0.101	0.036	0.036	0.954	0.001	0.001	0.036
	β_{23}	0.250	0.251	0.251	0.035	0.035	0.951	0.001	0.001	0.035
n=5000, 40% Censoring										
GH-BXII	η	1.250	1.240	1.237	0.066	0.067	0.949	-0.010	0.004	0.067
	ν	2.450	2.464	2.464	0.028	0.025	0.900	0.014	0.001	0.031
	δ	1.150	1.130	1.123	0.102	0.109	0.964	-0.020	0.011	0.103
	β_{11}	0.250	0.249	0.249	0.028	0.028	0.955	-0.001	0.001	0.028
	β_{12}	0.350	0.348	0.347	0.055	0.056	0.956	-0.002	0.003	0.055
	β_{13}	0.150	0.152	0.151	0.054	0.055	0.957	0.002	0.003	0.054
	β_{21}	0.150	0.151	0.151	0.023	0.023	0.950	0.001	0.001	0.023
	β_{22}	0.100	0.100	0.101	0.046	0.046	0.949	0.000	0.002	0.046
	β_{23}	0.250	0.249	0.249	0.045	0.045	0.951	-0.001	0.002	0.045

M.MLE: mean of the MLEs; **m.MLE:** median of the MLEs; **E.SD:** empirical standard deviation; **M.SE:** model-based standard error; **MSE:** mean-square error; **RMSE:** root-mean-square error; **Coverage:** coverage proportions.

Table 2: Simulation from the PH-1 Structure with (η, ν, δ) = (1.25, 2.20, 1.15), β = (0.15, 0.10, 0.25)

$h_{BXII}^{PH}(t; x_j) = h_{BXII}(t; 1.25, 2.20, 1.15) \times \exp(0.15{\times}age + 0.10{\times}sex + 0.25{\times}TRT)$.

Model	Parameters	TRUE	M.MLE	m.MLE	E.SD	M.SE	Coverage	Bias	MSE	RMSE
n=1000, 20% Censoring										
GH-BXII	η	1.250	1.214	1.203	0.128	0.135	0.954	-0.036	0.018	0.133
	ν	2.200	2.197	2.197	0.040	0.051	0.988	-0.003	0.002	0.040
	δ	1.150	1.075	1.056	0.169	0.194	0.963	-0.075	0.034	0.185
	β_{11}	0	0.000	-0.001	0.062	0.063	0.958	0.000	0.004	0.062
	β_{12}	0	0.001	0.000	0.125	0.125	0.953	0.001	0.016	0.125
	β_{13}	0	-0.002	-0.004	0.123	0.126	0.955	-0.002	0.015	0.123
	β_{21}	0.150	0.148	0.147	0.042	0.042	0.953	-0.002	0.002	0.042
	β_{22}	0.100	0.099	0.098	0.085	0.083	0.947	-0.001	0.007	0.085
	β_{23}	0.250	0.246	0.245	0.084	0.084	0.955	-0.004	0.007	0.084
PH-BXII	η	1.250	1.209	1.204	0.068	0.108	0.993	-0.041	0.006	0.080
	ν	2.200	2.193	2.193	0.042	0.050	0.981	-0.007	0.002	0.042
	δ	1.150	1.064	1.054	0.106	0.162	0.989	-0.086	0.019	0.137
	β_1	0.150	0147	0.147	0.036	0.036	0.949	-0.003	0.001	0.036
	β_2	0.100	0.099	0.099	0.073	0.071	0.945	-0.001	0.005	0.073
	β_3	0.250	0.245	0.245	0.072	0.072	0.952	-0.005	0.005	0.072
n=1000, 40% Censoring										
GH-BXII	η	1.250	1.263	1.240	0.188	0.173	0.941	0.013	0.036	0.189
	ν	2.200	2.181	2.180	0.056	0.056	0.935	-0.019	0.004	0.059
	δ	1.150	1.150	1.103	0.273	0.258	0.956	0.000	0.075	0.273
	β_{11}	0	0.001	0.002	0.079	0.079	0.954	0.001	0.006	0.079
	β_{12}	0	0.002	0.001	0.159	0.158	0.955	0.002	0.025	0.159
	β_{13}	0	0.001	-0.001	0.159	0.159	0.957	0.001	0.025	0.159
	β_{21}	0.150	0.148	0.146	0.056	0.056	0.954	-0.002	0.003	0.056
	β_{22}	0.100	0.097	0.097	0.114	0.110	0.945	-0.003	0.013	0.114
	β_{23}	0.250	0.245	0.243	0.112	0.110	0.953	-0.005	0.013	0.113
PH-BXII	η	1.250	1.247	1.236	0.112	0.136	0.984	-0.003	0.013	0.112
	ν	2.200	2.176	2.175	0.056	0.055	0.926	-0.024	0.004	0.061
	δ	1.150	1.117	1.097	0.168	0.206	0.986	-0.033	0.029	0.172
	β_1	0.150	0.148	0.147	0.042	0.042	0.948	-0.002	0.002	0.042
	β_2	0.100	0.098	0.098	0.084	0.082	0.944	-0.002	0.007	0.084
	β_3	0.250	0.245	0.245	0.083	0.083	0.951	-0.005	0.007	0.083
n=5000, 20% Censoring										
GH-BXII	η	1.250	1.228	1.226	0.056	0.061	0.949	-0.022	0.004	0.060
	ν	2.200	2.217	2.217	0.018	0.023	0.940	0.017	0.001	0.024
	δ	1.150	1.115	1.112	0.075	0.088	0.963	-0.035	0.007	0.083
	β_{11}	0	0.001	0.000	0.027	0.028	0.953	0.001	0.001	0.027
	β_{12}	0	0.000	0.001	0.055	0.056	0.956	0.000	0.003	0.055
	β_{13}	0	0.001	0.001	0.054	0.056	0.958	0.001	0.003	0.054
	β_{21}	0.150	0.149	0.149	0.019	0.019	0.954	-0.001	0.000	0.019
	β_{22}	0.100	0.099	0.099	0.038	0.038	0.952	-0.001	0.001	0.038
	β_{23}	0.250	0.249	0.249	0.038	0.038	0.953	-0.001	0.001	0.038

(Table2). Continued.

Model	Parameters	TRUE	M.MLE	m.MLE	E.SD	M.SE	Coverage	Bias	MSE	RMSE
PH-BXII	η	1.250	1.226	1.225	0.031	0.049	0.989	-0.024	0.002	0.039
	ν	2.200	2.216	2.216	0.019	0.022	0.932	0.016	0.001	0.025
	δ	1.150	1.112	1.110	0.050	0.074	0.984	-0.038	0.004	0.063
	β_1	0.150	0.149	0.150	0.016	0.016	0.951	-0.001	0.000	0.016
	β_2	0.100	0.099	0.099	0.032	0.032	0.951	-0.001	0.001	0.032
	β_3	0.250	0.250	0.249	0.032	0.032	0.951	0.000	0.001	0.032
n=5000, 40% Censoring										
GH-BXII	η	1.250	1.241	1.237	0.076	0.075	0.946	-0.009	0.006	0.077
	ν	2.200	2.212	2.212	0.025	0.025	0.921	0.012	0.001	0.028
	δ	1.150	1.134	1.127	0.108	0.113	0.957	-0.016	0.012	0.110
	β_{11}	0	0.001	0.001	0.034	0.035	0.954	0.001	0.001	0.034
	β_{12}	0	0.001	0.001	0.068	0.069	0.955	0.001	0.005	0.068
	β_{13}	0	0.003	0.003	0.067	0.069	0.959	0.003	0.004	0.067
	β_{21}	0.150	0.149	0.148	0.024	0.025	0.950	-0.001	0.001	0.024
	β_{22}	0.100	0.098	0.099	0.049	0.049	0.948	-0.002	0.002	0.049
	β_{23}	0.250	0.248	0.248	0.049	0.049	0.952	-0.002	0.002	0.049
PH-BXII	η	1.250	1.236	1.234	0.048	0.060	0.979	-0.014	0.003	0.050
	ν	2.200	2.210	2.210	0.026	0.025	0.917	0.010	0.001	0.028
	δ	1.150	1.126	1.123	0.074	0.093	0.982	-0.024	0.006	0.078
	β_1	0.150	0.150	0.149	0.018	0.018	0.952	0.000	0.000	0.018
	β_2	0.100	0.099	0.099	0.037	0.037	0.947	-0.001	0.001	0.037
	β_3	0.250	0.249	0.249	0.037	0.037	0.950	-0.001	0.001	0.037

M.MLE: mean of the MLEs; **m.MLE:** median of the MLEs; **E.SD:** empirical standard deviation; **M.SE:** model-based standard error; **MSE:** mean-square error; **RMSE:** root-mean-square error; **Coverage:** coverage proportions.

Overall, the AFT–BXII model consistently emerged as the best-fitting model across both AFT scenarios, with GH–BXII serving as a flexible alternative under misspecification (supplementary Tables **S15-S17**).

In the AH-1 and AH-2 structure, the AH–BXII model consistently provided the best fit to the simulated data, as confirmed by information criteria and graphical assessments (Tables **S1** and S18). The GH–BXII model performed comparably, reinforcing the interpretation of the AH framework as a special case of the generalized hazard model. In contrast, both PH–BXII and AFT–BXII systematically underestimated survival (Tables **4** and **S19-S20**). For example, under AH-1 structure in Table **4** with n=1000 and 20% censoring, the age effect (β_1) was estimated with minimal bias (–0.003) and RMSE of 0.055 in the AH–BXII model, compared with bias of 0.007 and RMSE of 0.058 in the GH–BXII model. Increasing censoring from 20% to 40% led to higher variability and larger RMSEs. For instance, the RMSE for δ in GH–BXII rose from 0.174 to 0.245 at n=1000, yet bias remained small. Larger sample sizes substantially improved accuracy, with empirical standard deviation and RMSEs reduced by more than half and coverage probabilities approaching 95%. Overall, the AH–BXII model showed optimal parameter recovery under its generating mechanism, while the GH–BXII model again demonstrated robustness under misspecification.

6.2. Scenario 2 Results

The simulation results from Scenario 2 (Figure **2**) demonstrate the remarkable flexibility of the GH-BXII model in accurately recovering true hazard patterns. Visually, the estimated hazard functions exhibit strong agreement with their true underlying shapes across all scenarios: successfully capturing the steady rise in risk for increasing hazards, the monotonically declining pattern for decreasing hazards, and the characteristic peak-and-decline structure for unimodal hazards.

This close visual correspondence is supported by numerically accurate parameter estimation. The estimates for all parameters, including the shape parameters (η, v, δ) governing hazard behavior and the regression coefficients (β), exhibit minimal bias and are consistently close to their true values. Furthermore, the variability of these estimates decreases substantially as the sample size increases, demonstrating the

Table 3: Simulation from AFT-1 Structure with (η, ν, δ) = (1.45, 2.10, 1.15), β = (0.10, 0.15, 0.20)

$h_{BXII}^{AFT}(t; x_j) = h_{BXII}(t\times \exp(0.10\times age + 0.15\times sex + 0.20\times TRT)\,; 1.45, 2.10, 1.15) \times \exp(0.10\times age + 0.15\times sex + 0.20\times TRT)$.

Model	Parameters	TRUE	M.MLE	m.MLE	E.SD	M.SE	Coverage	Bias	MSE	RMSE
n=1000, 20% Censoring										
GH-BXII	η	1.450	1.400	1.390	0.155	0.147	0.918	-0.050	0.027	0.163
	ν	2.100	2.107	2.106	0.037	0.053	0.994	0.007	0.001	0.038
	δ	1.150	1.069	1.051	0.167	0.201	0.972	-0.081	0.034	0.185
	β_{11}	0.100	0.100	0.101	0.064	0.064	0.951	0.000	0.004	0.064
	β_{12}	0.150	0.154	0.154	0.129	0.128	0.952	0.004	0.017	0.129
	β_{13}	0.200	0.203	0.203	0.128	0.128	0.952	0.003	0.016	0.128
	β_{21}	0.100	0.100	0.100	0.040	0.039	0.947	0.000	0.002	0.040
	β_{22}	0.150	0.149	0.148	0.080	0.078	0.944	-0.001	0.006	0.080
	β_{23}	0.200	0.197	0.196	0.079	0.078	0.951	-0.003	0.006	0.079
AFT-BXII	η	1.450	1.384	1.379	0.092	0.115	0.955	-0.066	0.013	0.114
	ν	2.100	2.106	2.105	0.037	0.053	0.994	0.006	0.001	0.037
	δ	1.150	1.043	1.037	0.080	0.149	0.989	-0.107	0.018	0.134
	β_1	0.100	0.100	0.100	0.027	0.027	0.954	0.000	0.001	0.027
	β_2	0.150	0.151	0.150	0.055	0.055	0.950	0.001	0.003	0.055
	β_3	0.200	0.199	0.200	0.054	0.055	0.952	-0.001	0.003	0.054
n=1000, 40% Censoring										
GH-BXII	η	1.45	1.465	1.436	0.226	0.184	0.906	0.015	0.052	0.227
	ν	2.1	2.085	2.085	0.052	0.057	0.960	-0.015	0.003	0.054
	δ	1.15	1.148	1.106	0.266	0.260	0.959	-0.002	0.071	0.266
	β_{11}	0.1	0.101	0.100	0.079	0.078	0.951	0.001	0.006	0.079
	β_{12}	0.15	0.157	0.155	0.158	0.157	0.951	0.007	0.025	0.158
	β_{13}	0.2	0.205	0.203	0.159	0.157	0.951	0.005	0.025	0.159
	β_{21}	0.1	0.100	0.099	0.050	0.048	0.949	0.000	0.002	0.050
	β_{22}	0.15	0.147	0.146	0.101	0.096	0.941	-0.003	0.010	0.101
	β_{23}	0.2	0.196	0.196	0.099	0.097	0.951	-0.004	0.010	0.099
AFT-BXII	η	1.450	1.436	1.425	0.137	0.140	0.953	-0.014	0.019	0.138
	ν	2.100	2.084	2.084	0.051	0.057	0.964	-0.016	0.003	0.053
	δ	1.150	1.100	1.086	0.136	0.185	0.991	-0.050	0.021	0.145
	β_1	0.100	0.100	0.100	0.029	0.029	0.952	0.000	0.001	0.029
	β_2	0.150	0.150	0.150	0.059	0.059	0.949	0.000	0.003	0.059
	β_3	0.200	0.199	0.200	0.058	0.059	0.953	-0.001	0.003	0.058
n=5000, 20% Censoring										
GH-BXII	η	1.450	1.418	1.415	0.068	0.066	0.928	-0.032	0.006	0.076
	ν	2.100	2.120	2.120	0.017	0.023	0.943	0.020	0.001	0.026
	δ	1.150	1.109	1.105	0.075	0.091	0.965	-0.041	0.007	0.086
	β_{11}	0.100	0.099	0.099	0.028	0.029	0.952	-0.001	0.001	0.028
	β_{12}	0.150	0.149	0.149	0.056	0.057	0.958	-0.001	0.003	0.056
	β_{13}	0.200	0.200	0.199	0.056	0.057	0.958	0.000	0.003	0.056
	β_{21}	0.100	0.100	0.100	0.018	0.017	0.949	0.000	0.000	0.018
	β_{22}	0.150	0.150	0.150	0.035	0.035	0.950	0.000	0.001	0.035
	β_{23}	0.200	0.200	0.201	0.035	0.035	0.950	0.000	0.001	0.035

(Table3). Continued.

Model	Parameters	TRUE	M.MLE	m.MLE	E.SD	M.SE	Coverage	Bias	MSE	RMSE
AFT-BXII	η	1.450	1.416	1.415	0.041	0.052	0.949	-0.034	0.003	0.053
	ν	2.100	2.120	2.120	0.016	0.023	0.945	0.020	0.001	0.026
	δ	1.150	1.106	1.104	0.038	0.069	0.991	-0.044	0.003	0.058
	β_1	0.100	0.100	0.100	0.012	0.012	0.953	0.000	0.000	0.012
	β_2	0.150	0.150	0.149	0.024	0.024	0.950	0.000	0.001	0.024
	β_3	0.200	0.200	0.200	0.023	0.024	0.953	0.000	0.001	0.023
n=5000, 40% Censoring										
GH-BXII	η	1.45	1.436	1.432	0.091	0.080	0.908	-0.014	0.009	0.092
	ν	2.1	2.113	2.113	0.023	0.025	0.942	0.013	0.001	0.026
	δ	1.15	1.131	1.124	0.106	0.115	0.965	-0.019	0.012	0.108
	β_{11}	0.1	0.100	0.100	0.034	0.034	0.952	0.000	0.001	0.034
	β_{12}	0.15	0.151	0.151	0.067	0.068	0.954	0.001	0.005	0.067
	β_{13}	0.2	0.202	0.201	0.067	0.068	0.957	0.002	0.004	0.067
	β_{21}	0.1	0.100	0.100	0.022	0.021	0.949	0.000	0.000	0.022
	β_{22}	0.15	0.149	0.149	0.044	0.043	0.946	-0.001	0.002	0.044
	β_{23}	0.2	0.199	0.199	0.043	0.043	0.951	-0.001	0.002	0.043
AFT-BXII	η	1.450	1.431	1.428	0.058	0.062	0.952	-0.019	0.004	0.061
	ν	2.100	2.113	2.113	0.023	0.025	0.943	0.013	0.001	0.026
	δ	1.150	1.122	1.119	0.059	0.084	0.988	-0.028	0.004	0.066
	β_1	0.100	0.100	0.100	0.013	0.013	0.953	0.000	0.000	0.013
	β_2	0.150	0.149	0.149	0.025	0.026	0.950	-0.001	0.001	0.025
	β_3	0.200	0.200	0.200	0.025	0.026	0.953	0.000	0.001	0.025

M.MLE: mean of the MLEs; **m.MLE:** median of the MLEs; **E.SD:** empirical standard deviation; **M.SE:** model-based standard error; **MSE:** mean-square error; **RMSE:** root-mean-square error; **Coverage:** coverage proportions.

Table 4: Simulation from the AH-1 Structure with (η, ν, δ) = (1.25, 2.20, 1.15), β = (-0.25, 0.35, -0.15)

$h_{BXII}^{AH}(t; x_j) = h_{BXII}(t\times \exp(-0.25\times age + 0.35\times sex\ - 0.15\times TRT)\,; 1.25, 2.20, 1.15).$

Model	Parameters	TRUE	M.MLE	m.MLE	E.SD	M.SE	Coverage	Bias	MSE	RMSE
n=1000, 20% Censoring										
GH-BXII	η	1.250	1.200	1.192	0.117	0.133	0.960	-0.050	0.016	0.127
	ν	2.200	2.207	2.206	0.040	0.053	0.986	0.007	0.002	0.041
	δ	1.150	1.054	1.037	0.148	0.188	0.969	-0.096	0.031	0.177
	β_{11}	-0.250	-0.243	-0.243	0.058	0.059	0.954	0.007	0.003	0.058
	β_{12}	0.350	0.340	0.339	0.117	0.117	0.951	-0.010	0.014	0.117
	β_{13}	-0.150	-0.147	-0.147	0.116	0.115	0.949	0.003	0.013	0.116
	β_{21}	0.000	-0.007	-0.008	0.039	0.039	0.947	-0.007	0.002	0.040
	β_{22}	0.000	0.011	0.011	0.078	0.076	0.943	0.011	0.006	0.079
	β_{23}	0.000	-0.005	-0.007	0.077	0.075	0.948	-0.005	0.006	0.077
AH-BXII	η	1.250	1.201	1.194	0.115	0.127	0.955	-0.049	0.016	0.125
	ν	2.200	2.207	2.206	0.042	0.053	0.981	0.007	0.002	0.043
	δ	1.150	1.054	1.044	0.119	0.163	0.974	-0.096	0.023	0.153
	β_1	-0.250	-0.247	-0.247	0.054	0.056	0.958	0.003	0.003	0.055
	β_2	0.350	0.346	0.345	0.110	0.111	0.953	-0.004	0.012	0.110
	β_3	-0.150	-0.149	-0.150	0.109	0.110	0.951	0.001	0.012	0.109

(Table 4). Continued.

Model	Parameters	TRUE	M.MLE	m.MLE	E.SD	M.SE	Coverage	Bias	MSE	RMSE
n=1000, 40% Censoring										
GH-BXII	η	1.250	1.254	1.233	0.171	0.166	0.954	0.004	0.029	0.171
	ν	2.200	2.181	2.181	0.056	0.057	0.941	-0.019	0.004	0.059
	δ	1.150	1.132	1.096	0.239	0.243	0.965	-0.018	0.058	0.240
	β_{11}	-0.250	-0.247	-0.247	0.072	0.072	0.950	0.003	0.005	0.073
	β_{12}	0.350	0.347	0.344	0.144	0.144	0.956	-0.003	0.021	0.144
	β_{13}	-0.150	-0.150	-0.152	0.143	0.141	0.952	0.000	0.020	0.143
	β_{21}	0.000	-0.004	-0.005	0.049	0.049	0.949	-0.004	0.002	0.050
	β_{22}	0.000	0.005	0.006	0.098	0.096	0.946	0.005	0.010	0.099
	β_{23}	0.000	-0.003	-0.004	0.096	0.094	0.946	-0.003	0.009	0.096
AH-BXII	η	1.250	1.247	1.233	0.155	0.152	0.953	-0.003	0.024	0.155
	ν	2.200	2.183	2.183	0.058	0.057	0.936	-0.017	0.004	0.060
	δ	1.150	1.115	1.094	0.174	0.198	0.976	-0.035	0.031	0.177
	β_1	-0.250	-0.250	-0.251	0.062	0.063	0.953	0.000	0.004	0.062
	β_2	0.350	0.351	0.350	0.124	0.126	0.954	0.001	0.015	0.124
	β_3	-0.150	-0.152	-0.153	0.123	0.124	0.955	-0.002	0.015	0.123
n=5000, 20% Censoring										
GH-BXII	η	1.250	1.224	1.223	0.052	0.060	0.957	-0.026	0.003	0.058
	ν	2.200	2.220	2.220	0.018	0.024	0.926	0.020	0.001	0.027
	δ	1.150	1.109	1.106	0.068	0.086	0.969	-0.041	0.006	0.079
	β_{11}	-0.250	-0.247	-0.247	0.025	0.026	0.952	0.003	0.001	0.026
	β_{12}	0.350	0.346	0.346	0.051	0.052	0.957	-0.004	0.003	0.051
	β_{13}	-0.150	-0.148	-0.148	0.050	0.051	0.954	0.002	0.003	0.050
	β_{21}	0.000	-0.002	-0.002	0.017	0.018	0.952	-0.002	0.000	0.017
	β_{22}	0.000	0.002	0.002	0.034	0.034	0.951	0.002	0.001	0.034
	β_{23}	0.000	-0.001	-0.001	0.034	0.034	0.951	-0.001	0.001	0.034
n=5000, 40% Censoring										
AH-BXII	η	1.250	1.225	1.223	0.051	0.057	0.948	-0.025	0.003	0.057
	ν	2.200	2.220	2.220	0.019	0.023	0.914	0.020	0.001	0.028
	δ	1.150	1.109	1.107	0.054	0.074	0.972	-0.041	0.005	0.068
	β_1	-0.250	-0.248	-0.248	0.024	0.024	0.956	0.002	0.001	0.024
	β_2	0.350	0.347	0.347	0.048	0.049	0.956	-0.003	0.002	0.048
	β_3	-0.150	-0.149	-0.149	0.047	0.048	0.954	0.001	0.002	0.047
GH-BXII	η	1.250	1.238	1.235	0.070	0.073	0.958	-0.012	0.005	0.071
	ν	2.200	2.212	2.213	0.025	0.026	0.934	0.012	0.001	0.028
	δ	1.150	1.129	1.122	0.097	0.108	0.970	-0.021	0.010	0.099
	β_{11}	-0.250	-0.247	-0.248	0.031	0.031	0.952	0.003	0.001	0.031
	β_{12}	0.350	0.346	0.347	0.062	0.063	0.954	-0.004	0.004	0.062
	β_{13}	-0.150	-0.148	-0.148	0.060	0.061	0.956	0.002	0.004	0.060
	β_{21}	0.000	-0.001	-0.002	0.021	0.022	0.953	-0.001	0.000	0.021
	β_{22}	0.000	0.001	0.001	0.043	0.042	0.949	0.001	0.002	0.043
	β_{23}	0.000	-0.001	-0.001	0.042	0.042	0.950	-0.001	0.002	0.042
AH-BXII	η	1.250	1.237	1.235	0.064	0.066	0.953	-0.013	0.004	0.065
	ν	2.200	2.213	2.213	0.026	0.025	0.920	0.013	0.001	0.028
	δ	1.150	1.127	1.124	0.074	0.088	0.974	-0.023	0.006	0.077
	β_1	-0.250	-0.249	-0.249	0.026	0.027	0.956	0.001	0.001	0.026
	β_2	0.350	0.347	0.347	0.053	0.054	0.953	-0.003	0.003	0.053
	β_3	-0.150	-0.149	-0.149	0.052	0.054	0.957	0.001	0.003	0.052

M.MLE: mean of the MLEs; **m.MLE:** median of the MLEs; **E.SD:** empirical standard deviation; **M.SE:** model-based standard error; **MSE:** mean-square error; **RMSE:** root-mean-square error; **Coverage:** coverage proportions.

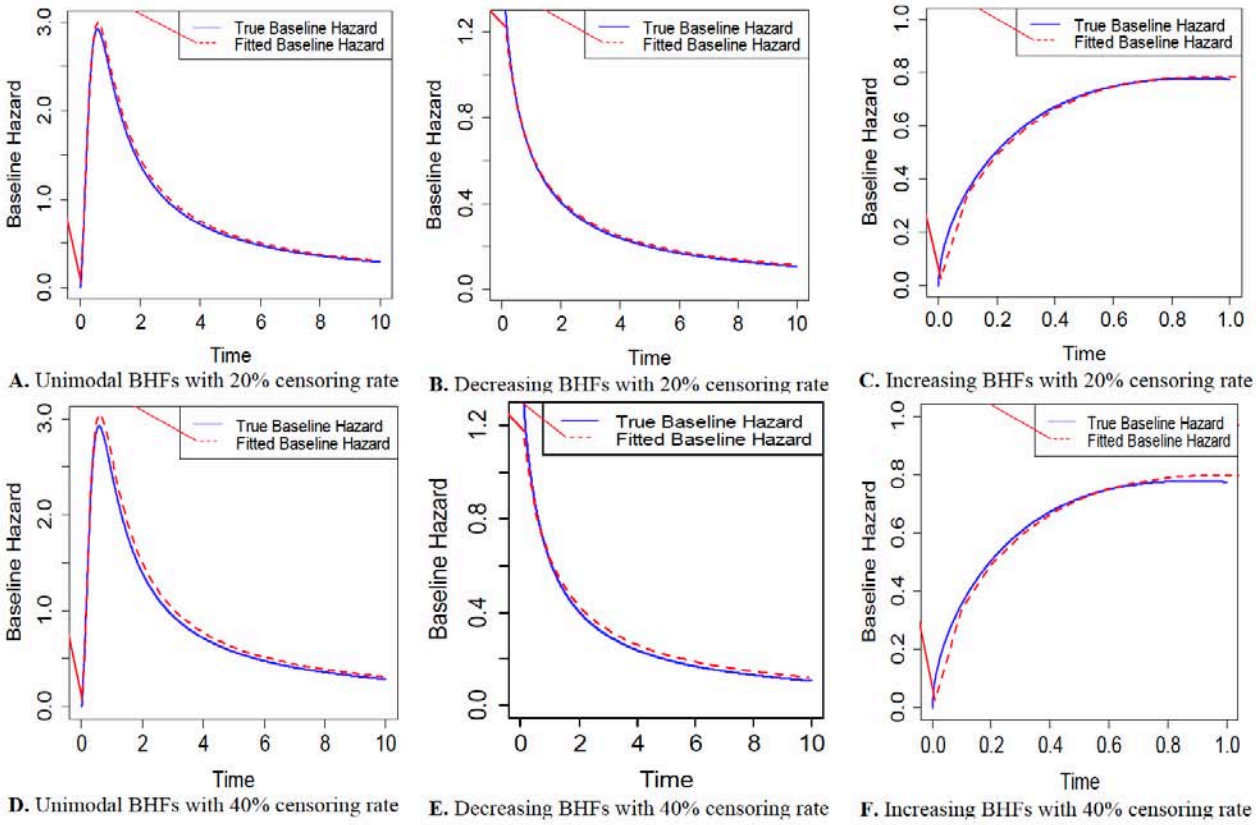

Figure 2: Recovered hazard rate functions under the GH-BXII model for three true hazard shapes (unimodal, decreasing, increasing) with n = 1000. Top row (20% censoring): (**A**) Unimodal, (**B**) Decreasing, (**C**) Increasing. Bottom row (40% censoring): (**D**) Unimodal, (**E**) Decreasing, (**F**) Increasing.

asymptotic consistency of the ML estimators. The model maintains this strong estimation performance even under moderate to high censoring rates (20% and 40%), highlighting its robustness (Table **5**). This supplementary analysis highlights its ability to adaptively represent diverse hazard shapes beyond the constraints of conventional proportional hazards or accelerated failure time models. Consequently, it emerges as a powerful and robust parametric tool for survival analysis where the underlying hazard shape is unknown a priori and must be discovered empirically from the data.

The coverage probability for the shape parameter v was slightly below the nominal level in some scenarios, particularly under heavier censoring (e.g., Table **1**: 0.900 at n=5000, 40% censoring). This behavior reflects two factors. First, v primarily controls the tail behavior of the Burr XII distribution; censoring removes tail observations, thereby reducing the effective information available for precise estimation of this parameter. Second, Wald-type confidence intervals for v rely on asymptotic normality of the MLE, whereas the finite-sample distribution of $\hat{v}$ remains moderately skewed under censoring, leading to mild under coverage. This pattern is not attributable to numerical instability, as the Hessian was operationally invertible in all reported replicates (Supplementary Table **S21**). For applied researchers: under 20% censoring, n=1000 provides adequate performance; under 40% censoring, larger samples (n≥5000) are preferable if inference on v is a primary objective. When the primary focus is on regression coefficients, the model remains reliable, but interval estimates for v should be interpreted with additional caution.

7. REAL DATA EXAMPLE

7.1. Acute Myeloid Leukemia (AML) Dataset

The emergence of new therapeutic agents, alongside improvements in supportive care strategies, has greatly improved clinical outcomes after allogeneic hematopoietic stem cell transplantation (allo-HSCT) [9]. Strong clinical data repeatedly show that allo-HSCT is the most efficacious treatment option post-remission for preventing disease relapse among patients with acute myeloid leukemia (AML) [10]. In this retrospective cohort study, we analyzed 801 complete survival data from acute myeloid leukemia (AML) patients who underwent allo-HSCT at the research and hematology center of Shariati Hospital in Tehran between 2008 and 2019 to predict post-transplant survival outcomes. This study was approved by the Ethics Committee of the Tehran University of Medical Sciences (approval ID: IR.TUMS.SPH.REC.1402.341). Informed consent was provided according to the Declaration of Helsinki. Since we have used secondary

Table 5: Simulation Results for Scenario 2 with about 20% and 40% Censoring Rates Based on GH Structure

Decreasing		n=1000								n=5000							
		20% Censoring				40% Censoring				20% Censoring				40% Censoring			
	True.p*	Mean	Med	2.5%	97.5%	Mean	Med	2.5%	97.5%	Mean	Med	2.5%	97.5%	Mean	Med	2.5%	97.5%
η	0.90	1.013	0.908	0.474	2.202	1.150	0.900	0.359	5.088	0.916	0.897	0.667	1.259	0.933	0.897	0.599	1.457
ν	0.95	0.954	0.952	0.860	1.057	0.956	0.952	0.851	1.074	0.950	0.949	0.908	0.995	0.950	0.949	0.902	1.001
δ	1.25	1.328	1.267	0.821	2.162	1.429	1.263	0.662	3.471	1.261	1.250	1.029	1.545	1.275	1.253	0.946	1.722
β_{11}	-0.35	-0.357	-0.356	-0.665	-0.049	-0.376	-0.357	-0.801	0.049	-0.351	-0.351	-0.486	-0.216	-0.357	-0.349	-0.539	-0.175
β_{12}	0.55	0.577	0.565	-0.037	1.192	0.597	0.560	-0.264	1.459	0.547	0.542	0.278	0.815	0.550	0.537	0.187	0.912
β_{13}	-0.15	-0.152	-0.139	-0.734	0.430	-0.170	-0.146	-0.975	0.635	-0.150	-0.152	-0.406	0.106	-0.154	-0.149	-0.499	0.192
β_{21}	0.25	0.251	0.249	0.110	0.392	0.247	0.247	0.088	0.406	0.250	0.250	0.187	0.312	0.248	0.248	0.179	0.318
β_{22}	-0.45	-0.445	-0.449	-0.734	-0.155	-0.441	-0.447	-0.770	-0.111	-0.453	-0.455	-0.581	-0.325	-0.453	-0.454	-0.597	-0.309
β_{23}	0.55	0.555	0.555	0.277	0.832	0.550	0.551	0.236	0.865	0.552	0.551	0.428	0.675	0.551	0.551	0.412	0.689
Increasing		20% Censoring				40% Censoring				20% Censoring				40% Censoring			
η	1.30	1.359	1.308	0.861	2.158	1.409	1.306	0.763	2.698	1.307	1.298	1.076	1.588	1.315	1.292	1.025	1.689
ν	1.55	1.558	1.555	1.404	1.728	1.559	1.556	1.390	1.748	1.550	1.551	1.480	1.624	1.551	1.549	1.474	1.632
δ	1.25	1.315	1.263	0.816	2.131	1.383	1.265	0.703	2.860	1.259	1.249	1.029	1.540	1.269	1.249	0.968	1.664
β_{11}	0.15	0.150	0.146	-0.031	0.331	0.141	0.139	-0.089	0.371	0.149	0.150	0.070	0.229	0.148	0.148	0.048	0.248
β_{12}	-0.30	-0.309	-0.306	-0.673	0.055	-0.322	-0.307	-0.791	0.147	-0.305	-0.307	-0.465	-0.145	-0.309	-0.306	-0.510	-0.108
β_{13}	0.55	0.565	0.560	0.184	0.947	0.577	0.564	0.079	1.076	0.550	0.548	0.384	0.717	0.554	0.553	0.343	0.765
β_{21}	0.40	0.402	0.400	0.330	0.473	0.403	0.402	0.318	0.488	0.400	0.399	0.368	0.432	0.400	0.400	0.363	0.437
β_{22}	0.30	0.304	0.304	0.160	0.448	0.307	0.308	0.137	0.478	0.299	0.299	0.235	0.363	0.300	0.300	0.226	0.374
β_{23}	-0.20	-0.202	-0.202	-0.349	-0.055	-0.208	-0.206	-0.384	-0.032	-0.199	-0.200	-0.264	-0.134	-0.200	-0.201	-0.276	-0.124
Unimodal		20% Censoring				40% Censoring				20% Censoring				40% Censoring			
η	0.50	0.511	0.504	0.396	0.658	0.517	0.504	0.374	0.717	0.501	0.499	0.449	0.560	0.503	0.499	0.438	0.578
ν	2.40	2.408	2.408	2.167	2.677	2.409	2.403	2.142	2.710	2.399	2.400	2.289	2.515	2.399	2.398	2.277	2.527
δ	1.20	1.253	1.207	0.844	1.862	1.292	1.211	0.765	2.198	1.208	1.201	1.019	1.433	1.216	1.200	0.974	1.517
β_{11}	0.65	0.652	0.652	0.548	0.756	0.653	0.651	0.526	0.779	0.650	0.649	0.604	0.696	0.651	0.651	0.595	0.707
β_{12}	0.45	0.454	0.450	0.252	0.655	0.454	0.452	0.214	0.695	0.448	0.447	0.359	0.537	0.447	0.446	0.341	0.553
β_{13}	0.55	0.552	0.553	0.350	0.754	0.552	0.549	0.311	0.794	0.549	0.549	0.460	0.638	0.550	0.552	0.444	0.657
β_{21}	0.35	0.348	0.348	0.268	0.427	0.348	0.347	0.247	0.449	0.349	0.350	0.314	0.385	0.349	0.349	0.305	0.393
β_{22}	0.15	0.148	0.149	-0.001	0.298	0.147	0.147	-0.037	0.330	0.149	0.149	0.083	0.215	0.149	0.149	0.069	0.230
β_{23}	0.25	0.249	0.252	0.099	0.399	0.246	0.248	0.061	0.431	0.251	0.250	0.185	0.318	0.251	0.249	0.170	0.332

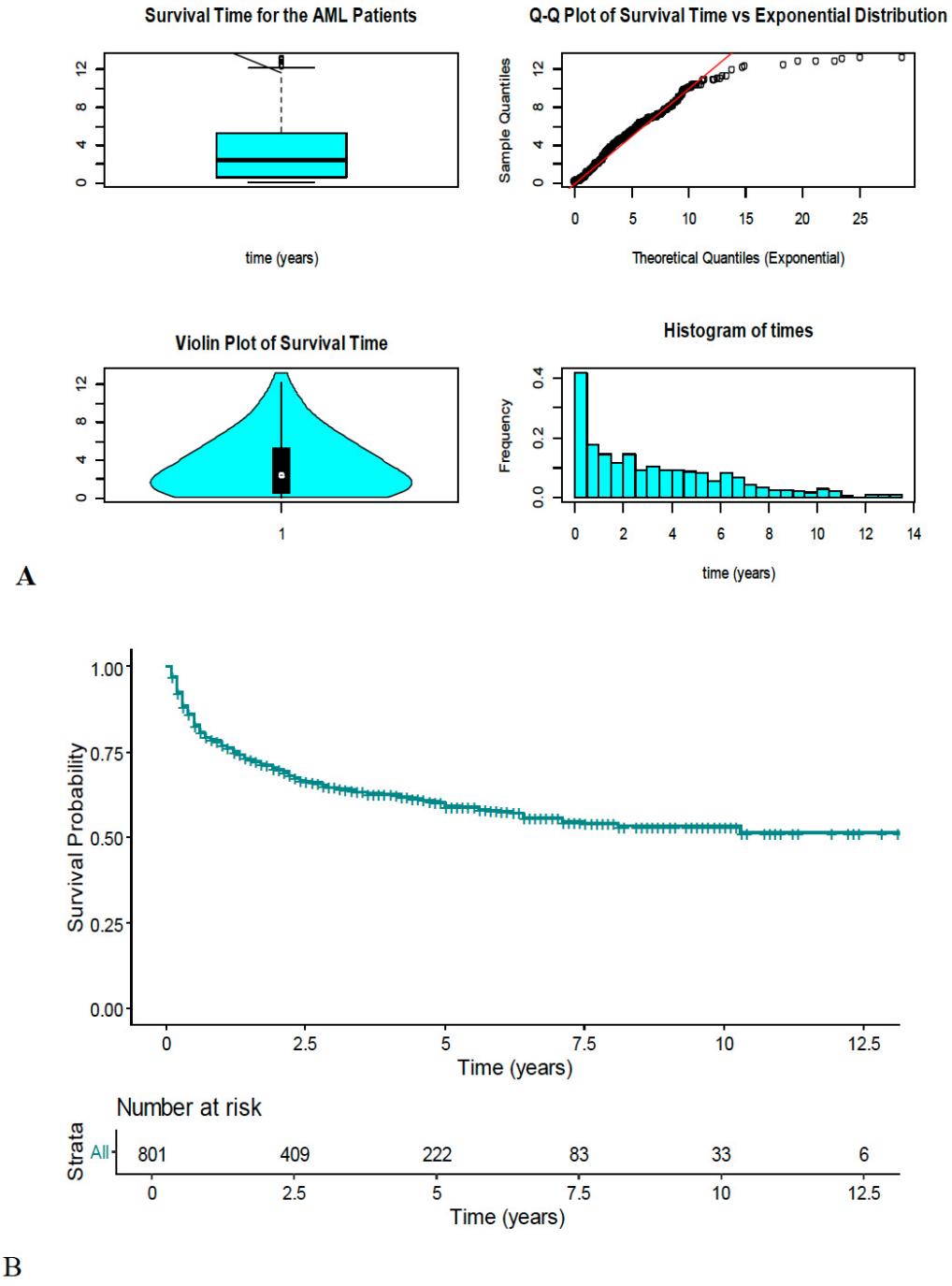

Figure 3: Non-parametric plots for the survival time data of AML cancer patients (**A**); The overall survival curve (**B**).

data, none of the authors had direct access to the patients, and this research complied with ethical standards. The real data used in this study was accessed for research purposes on November 25, 2024.

AML, a hematologic malignancy marked by the rapid proliferation of abnormal myeloid cells in the bone marrow, is among the most common acute leukemias. Allo-HCT remains a critical treatment for AML patients, particularly those with high-risk or relapsed disease, though numerous prognostic factors influence post-transplant survival [11]. While AML is rare in individuals under 45 years of age, it can occur in children and is slightly more prevalent in males, with a lifetime risk of approximately 0.5% for both sexes [12].

Using the AML dataset, we evaluate whether covariates exhibit time-dependent, proportional, or both effects on survival time. To refine survival predictions, we implement a flexible baseline hazard framework based on the three-parameter Burr XII (BXII) distribution. This approach enables nuanced characterization of baseline hazard patterns, offering

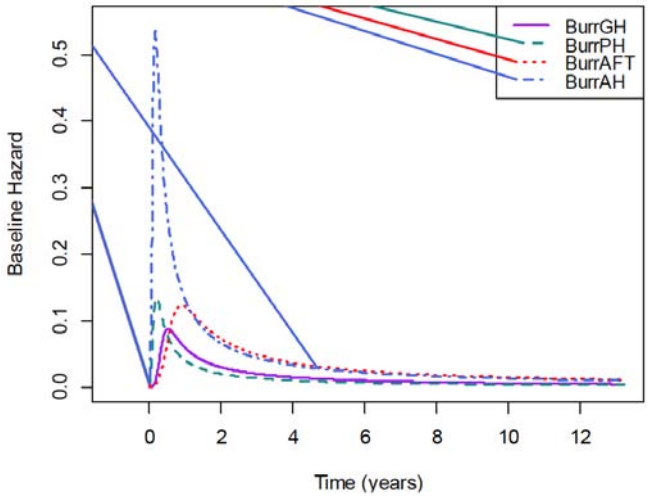

Figure 4: Estimated baseline hazards for the competitive models of the AML cancer patients.

actionable insights into survival trends for AML patients post allo-HSCT. Prognostic factors assessed for survival time of AML patients include: age at transplant, time from diagnosis to HSCT (diagnosis to HSCT time), occurrence of graft-versus-host disease (aGVHD), and disease status at transplantation (CR1, CR2, CR3), which can affect a patient's prognosis following allo-HSC. All analyses were conducted using R statistical software. The covariate "time from diagnosis to HSCT" was analyzed as a binary variable using a cutoff of 0.6 years, which corresponded to the sample median in the study population.

The fundamental non-parametric plots and Kaplan–Meier survival curves characterizing survival outcomes in acute myeloid leukemia (AML) patients are presented in Figures **3A** and **3B**.

The mean follow-up duration for censored patients was 4.4 years, and the median follow-up time for overall survival was 2.4 years (range: 35 days to 13.1 years). The 25th, 50th, and 75th percentiles of the patients' ages at diagnosis were 26.5, 35.6, and 45.1 years, with a mean age of 36.2 years. The median time from diagnosis to allo-HSCT was 0.6 years, with 38.2% of patients.

HSCT within <0.6 years of diagnosis and 61.8% exceeding this interval. At the time of HSCT, 74.1% of patients were in first complete remission (CRI), 20.4%

Table 6: Maximum Likelihood (SE) Estimates of the Parameters for the Fitted Models, with their Corresponding AIC and AICc

Model		PH-BXII		GH-BXII		AFT-BXII		AH-BXII	
		MLE (SE)	P value	MLE (SE)	P value	MLE (SE)	P value	MLE (SE)	P value
Scale		-1.83 (0.12)	0.187	-0.92 (0.54)	0.462	-0.38 (0.54)	0.206	-2.01 (0.50)	0.789
Shape1		1.14 (0.18)	<0.0001	1.46 (0.29)	<0.0001	1.40 (0.25)	<0.0001	1.20 (0.21)	<0.0001
Shape2		-4.35 (0.50)	0.979	-4.26 (0.60)	0.981	-3.31 (0.29)	0.900	-3.22 (0.49)	0.935
Age_t (years)		-	-	-0.01 (0.01)	0.413	0.01 (0.06)	0.882	-0.01 (0.01)	0.127
aGVHD_t	No	Ref	-	Ref	-	Ref	-	Ref	-
	Yes	-	-	0.06 (0.19)	0.758	-0.11 (0.15)	0.484	0.32 (0.15)	0.039
Diag to HSCT_t	<0.6	Ref	-	Ref	-	Ref	-	Ref	-
	≥0.6	-	-	0.49 (0.19)	0.008	0.41 (0.16)	0.010	0.17 (0.15)	0.250
CR_t	CR1	Ref	-	Ref	-	Ref	-	Ref	-
	CR2	-	-	0.11 (0.19)	0.553	0.37 (0.18)	0.042	-0.20 (0.15)	0.182
	CR3	-	-	0.18 (0.27)	0.498	0.48 (0.28)	0.089	-0.23 (0.25)	0.345
Age		0.01 (0.01)	0.175	0.01 (0.01)	0.609	-[a]	-	-	-
aGVHD	No	Ref	-	-	-	-[a]	-	-	-
	Yes	-0.28 (0.14)	0.045	-0.25 (0.18)	0.173	-[a]	-	-	-
Diag to HSCT	<0.6	Ref	-	-	-	-[a]	-	-	-
	≥0.6	0.07 (0.13)	0.593	0.37 (0.17)	0.030	-[a]	-	-	-
CR	CR1	Ref	-	-	-	-[a]	-	-	-
	CR2	0.51 (0.14)	<0.0001	0.57 (0.18)	0.002	-[a]	-	-	-
	CR3	0.66 (0.23)	0.005	0.75 (0.28)	0.008	-[a]	-	-	-
AIC		1669.682		1667.714		1673.465		1683.510	
AICc		1669.864		1668.176		1673.647		1683.692	

Note: The time-dependent effects are indicated with the subindex "_t"; β_t (time-dependent component) and β_h (proportional hazard component); [a] The AFT model assumes covariate effects are identical for time-dependent and time-fixed variables by design; The lowest information criterion value is highlighted in bold. Ref: Reference category.

Table 7: LRT Test for the GH Model and its Sub-Models

Model	Hypothesis	LRT Statistic	P-Value
GH-BXII vs. PH-BXII	H_0: β_2= 0, H_1: H_0 is false,	11.968	0.035
GH-BXII vs. AH-BXII	H_0: β_1= 0, H_1: H_0 is false,	25.796	< 0.001
GH-BXII vs. AFT-BXII	H_0: β_2= β_1, H_1: H_0 is false,	15.751	0.008

in CR2, and 5.5% in CR3, while 25.2% experienced acute graft-versus-host disease (aGVHD).

As shown in Table **5**, the GH model exhibits the lowest AIC value, indicating a superior statistical fit to the data. However, the GH model demonstrates enhanced versatility by accommodating time-dependent covariate effects and enabling selection among its submodels (PH, AH, and AFT). The estimated BHF for the competitive models is given in Figure **4**.

The GH model showed that in patients with a diagnosis time to allo-HSCT of more than 0.6 years (7 months), the speed of the death event is exp(0.49) = 1.63 times that of patients with a diagnosis time to allo-HSCT of less than 0.6 years. This means that increasing the time interval from diagnosis to transplant by more than 0.6 years causes an increased risk of death over time (harmful effect) (p=0.008). Patients with a diagnostic time to allo-HSCT of more than 0.6 years (exp(0.37) = 1.45) have a 45% higher instantaneous risk of death than those with a diagnostic time to allo-HSCT of less than 0.6 years during the study period. The AML patients in the CR2 category faced a higher hazard of death than those in CR1 (HR = 1.77, p = 0.002), and patients in the CR3 category had over double the death hazard compared to CR1 (HR = 2.12, p = 0.008).

It is important to note that the GH-BXII model allows for a flexible covariate structure, where an effect can be specified as either a time-fixed proportional hazard component (β_h) or a time-dependent log-acceleration component (β_t). In Table **6**, we compare several nested specifications. For the Diag to HSCT_t covariate, the GH-BXII column presents the estimated coefficient for the time-dependent effect (β_t), as this structure provided the best fit. In contrast, the PH-BXII column reports the coefficient for the time-fixed effect (β_h), as the PH-BXII model, by definition, excludes the time-dependent component. Thus, the coefficients in these columns correspond to different model specifications, rather than a single model simultaneously estimating both effects for the same variable.

Although the AIC difference between GH-BXII and PH-BXII is modest (ΔAIC = 1.97), the GH model nests the PH model (PH corresponds to β_2 = 0). The LRT for GH vs. PH yielded $\chi^2(5) = 11.97$ (p = 0.035), indicating a statistically significant improvement in fit at the α = 0.05 level (Table **7**). Similarly, GH significantly outperformed AFT (p = 0.008) and AH (p < 0.001).

8. DISCUSSION

This study introduces a GH regression model that integrates the structural frameworks of the PH, AFT, and AH models with the BXII baseline hazard distribution. The proposed GH-BXII model demonstrates strong predictive performance and provides a unified and flexible framework for selecting among its nested sub-models (PH-BXII, AFT-BXII, and AH-BXII). Simulation studies underscore a principal advantage of the GH-BXII model, such as its capacity to accurately capture a broad spectrum of underlying hazard shapes, including monotone (increasing, decreasing) and non-monotone (unimodal) patterns.

Our comprehensive simulation results demonstrate that the proposed GH-BXII model effectively handles time-independent and time-dependent covariates across varying censoring rates. Parameter estimates exhibited minimal finite-sample bias and converged toward their true values with increasing sample size, confirming the statistical consistency of the ML estimators. Notably, the model maintained robust performance under moderate to high censoring rates (20–40%), which illustrates the superiority of the GH-BXII model in real-world applications with incomplete data compared to other implementations.

Our work complements Muse *et al*. [3] by focusing on the Burr XII special case with a full frequentist maximum likelihood implementation, demonstrating its practical identifiability and robustness in smaller samples (n=1000) and for a different cancer type (AML). In general, the flexibility of the GH-BXII model presents an impressive opportunity for public health and epidemiological research. In large-scale population-based survival studies where high censoring rates and complex, non-standard hazard shapes are often present, the GH model is an effective exploratory analytical method when the true hazard pattern is not known. Utilizing a single flexible parametric modeling application that simultaneously accommodates time-independent and time-dependent

covariates also allowed the model to adequately model heterogeneous hazard profiles across subgroups, making it a good fit for large epidemiological datasets [1, 3]. In epidemiological research, socio-demographic factors, intervention effectiveness, and comorbidities usually have effects that change over time, and the GH-BXII model allows for a more accurate estimation of risk, which can help fill critical knowledge gaps in public health policy and interventions.

These findings indicate that the GH-BXII model offers a reliable analytical framework for survival data, especially in cancer epidemiology, where the hazard function is right-skewed. The model's proficiency in identifying non-monotonic hazards (e.g., a peak in recurrence risk followed by a decline) is particularly relevant in oncology. Empirical validation using a real dataset confirmed the practical utility of the model. As evidenced by lower information criteria, the GH-BXII specification exhibited superior fit over submodels (PH-BXII, AFT-BXII, AH-BXII), solidifying its value in applied research. The simulation results provide empirical evidence supporting the asymptotic properties of the MLEs. Under all scenarios, increasing the sample size reduced bias and variability, and coverage probabilities remained close to 95%, confirming that the normal approximation is adequate for practical sample sizes.

An important consideration in flexible parametric general hazard models is the identifiability and stability of parameter estimation, particularly when both hazard scale and time scale covariate effects are estimated simultaneously alongside multiple baseline hazard parameters. In the proposed GH–BXII framework, the baseline distribution parameters and the regression components enter the hazard function through structurally distinct mechanisms, which helps reduce direct confounding between the shape of the baseline hazard and the covariate effects.

From a theoretical perspective, the MLEs satisfy the standard asymptotic properties of consistency and asymptotic normality under regularity conditions commonly assumed in parametric survival analysis with independent censoring. Although deriving closed-form expressions for the expected Fisher information matrix is analytically difficult because of the complexity of the GH structure and the BXII baseline hazard, the observed information matrix provided stable variance estimation across the simulation settings considered in this study.

The simulation results further suggest that the proposed model is practically identifiable under moderate to large sample sizes and censoring levels. Bias and RMSE generally decreased with increasing sample size, and the empirical coverage probabilities remained close to their nominal values across most scenarios. Nevertheless, as with many highly parameterized flexible survival models, estimation of shape-related parameters may become less stable in smaller samples or under heavier censoring. Therefore, caution is warranted when fitting the full GH–BXII model in limited data settings, and simpler nested structures such as PH, AFT, or AH may be preferable when supported by the data.

9. CONCLUSION

In conclusion, the proposed model introduced in this paper provides a versatile and robust parametric framework for survival analysis. It effectively synthesizes several common regression structures while extending the capability to model diverse hazard shapes and complex covariate effects. Supported by extensive simulations and an empirical application, the GH-BXII model is particularly well-suited for settings where the underlying hazard form is unknown or complex, and where censoring is substantial.

Future research will extend the model to accommodate more complex data structures, such as interval- or left-censoring, and mixture models with cure fractions. Further methodological work could explore Bayesian estimation strategies and machine learning extensions for high-dimensional covariate spaces.

DATA AVAILABILITY

The data will be made available if requested by the researcher via email to the corresponding author of the article.

ETHICAL APPROVAL AND CONSENT TO PARTICIPATE

This study was found to be under the ethical principles and the national norms and standards for conducting medical research in Iran by the research ethics committee of the school of public health & allied medical sciences Tehran university of medical sciences. The approval ID is IRIR.TUMS.SPH.REC. 1402.341.

FUNDING

This research did not receive any specific grant from funding agencies in the public, commercial, or not-for-profit sectors.

ACKNOWLEDGEMENTS

This study is a part of the research process supported by the Tehran University of Medical Science to achieve a Ph.D degree.

The authors used AI solely for grammatical and spelling corrections to improve the readability of the manuscript. No generative AI was used to produce content.

CONFLICT OF INTEREST

The authors declare that they have no known competing financial interests or personal relationships that could have appeared to influence the work reported in this paper.

AUTHOR CONTRIBUTIONS

Conceptualization: S. Dalvand, M. Yaseri

Data curation: A. Kasaeian, S. Rostami, M. Vaezi

Formal analysis & Software: S. Dalvand

Investigation: S. Dalvand, M. Yaseri, H. Zeraati, A. Kasaeian, M. Vaezi

Methodology: S. Dalvand, M. Yaseri, H. Zeraati

Project administration & Supervision: M. Yaseri, H. Zeraati

Validation: M. Yaseri, A. Kasaeian, M. Vaezi, S. Rostami

Visualization: S. Dalvand

Writing, original draft: S. Dalvand

Writing, review & editing: M. Yaseri, H. Zeraati, A. Kasaeian, M. Vaezi, S. Rostami

SUPPLEMENTARY TABLES

The supplementary table can be downloaded from the journal website along with the article.

REFERENCES

[1] Rubio FJ, Remontet L, Jewell NP, Belot A. On a general structure for hazard-based regression models: an application to population-based cancer research. Statistical Methods in Medical Research 2019; 28(8): 2404-17. https://doi.org/10.1177/0962280218782293

[2] Chen YQ, Jewell NP. On a general class of semiparametric hazards regression models. Biometrika 2001; 88(3): 687-702. https://doi.org/10.1093/biomet/88.3.687

[3] Muse AH, Mwalili S, Ngesa O, Chesneau C, Al-Bossly A, El-Morshedy M. Bayesian and Frequentist Approaches for a Tractable Parametric General Class of Hazard-Based Regression Models: An Application to Oncology Data. Mathematics 2022; 10(20): 3813. https://doi.org/10.3390/math10203813

[4] Burr IW. Cumulative frequency functions. The Annals of Mathematical Statistics 1942; 13(2): 215-32. https://doi.org/10.1214/aoms/1177731607

[5] Bender R, Augustin T, Blettner M. Generating survival times to simulate Cox proportional hazards models. Statistics in Medicine 2005; 24(11): 1713-23. https://doi.org/10.1002/sim.2059

[6] Leemis LM, Shih L-H, Reynertson K. Variate generation for accelerated life and proportional hazards models with time dependent covariates. Statistics & Probability Letters 1990; 10(4): 335-9. https://doi.org/10.1016/0167-7152(90)90052-9

[7] Muse AH, Ngesa O, Mwalili S, Alshanbari HM, El-Bagoury A-AH. A Flexible Bayesian Parametric Proportional Hazard Model: Simulation and Applications to Right-Censored Healthcare Data. Journal of Healthcare Engineering 2022; 2022(1): 2051642. https://doi.org/10.1155/2022/2051642

[8] Rubio FJ, Rachet B, Giorgi R, Maringe C, Belot A. On models for the estimation of the excess mortality hazard in case of insufficiently stratified life tables. Biostatistics 2021; 22(1): 51-67. https://doi.org/10.1093/biostatistics/kxz017

[9] Niederwieser D, Baldomero H, Szer J, Gratwohl M, Aljurf M, Atsuta Y, *et al*. Hematopoietic stem cell transplantation activity worldwide in 2012 and a SWOT analysis of the Worldwide Network for Blood and Marrow Transplantation Group including the global survey. Bone Marrow Transplantation 2016; 51(6): 778-85. https://doi.org/10.1038/bmt.2016.18

[10] Döhner H, Wei AH, Appelbaum FR, Craddock C, DiNardo CD, Dombret H, *et al*. Diagnosis and management of AML in adults: 2022 recommendations from an international expert panel on behalf of the ELN. Blood 2022; 140(12): 1345-77. https://doi.org/10.1182/blood.2022016867

[11] Jimbu L, Valeanu M, Trifa AP, Mesaros O, Bojan A, Dima D, *et al*. A survival analysis of acute myeloid leukemia patients treated with intensive chemotherapy: a single center experience. Cureus 2023; 15(8). https://doi.org/10.7759/cureus.43794

[12] Key Statistics for Acute Myeloid Leukemia (AML) [Internet]. 2025 [cited 10 March 2025]. Available from: https://www.cancer.org/cancer/types/acute-myeloid-leukemia/about/key-statistics.html

Received on 09-05-2026 Accepted on 07-06-2026 Published on 01-07-2026

https://doi.org/10.6000/1929-6029.2026.15.26